Methane Conversion Using a High-Frequency Pulsed Plasma: Discharge Features

Shuiliang Yao, Akira Nakayama, and Eiji Suzuki
Catalysis Science Laboratory, Research Institute of Innovative Technology for the Earth, Kyoto 619-0292, Japan

The pulsed plasma of methane was experimentally characterized using single and sequential pulse modes. At a single pulse mode, only pulsed corona and streamer discharges occurred at a low pulse voltage. A pulsed spark discharge developed after the pulsed streamer discharge at a high pulse voltage. An image analysis indicated that the weak luminescence could be found in the latter period of the pulsed corona discharge. The pulsed streamer and spark discharges bridged the discharge gap and emitted a relatively strong light. At a sequential pulse mode, the streamer or spark discharge developed easily and evenly at a low pulse voltage, as the pulse frequency increased in comparison with that at the single pulse mode. The high-frequency pulsed plasma was more practical than other plasmas due to its relatively high energy efficiency at room temperature and atmospheric pressure.

Introduction

Nonthermal plasma processing is an emerging advanced technology for environmental and other applications (Chang, 1993; Potakin et al., 1993; Penetrante et al., 1997; Thanyachotpaiboon et al., 1998). Nonthermal pulsed plasma has a relatively high energy efficiency since the majority of electric energy in a pulsed plasma is utilized for the production of energetic electrons that activate background gas, rather than for heating. This technology has been widely studied for applications such as removal of NO_x and SO_x from combustion flue gas and destruction of organic compound in wastes (Eliasson and Kogelschatz, 1991b; Rea and Yan, 1993; Mutaf-Yardimchi et al., 1998; Oda et al., 1998; Puchkarev et al., 1998; Smulders et al., 1998; Sun et al., 1999; Urashima et al., 1999). A successful process of a nonthermal plasma process is the ozone generation system that was developed by Siemens 100 years ago (Horvath et al., 1985).

In order to produce active ions and electrons for advanced manufacturing processes, the power supply equipment yields a high pulse voltage with a short rise time and long duration period. Such a type of pulse power supply is costly in general with a low electric energy efficiency. The improvement of electric efficiency and production of higher value materials are required for its practical use in industry.

On the other hand, studies on the formation of plasmas, such as streamer discharge, have been performed for several decades (Dawson and Winn, 1965; Geary and Penney, 1978; Sigmond, 1984; Dhali and Williams, 1985, 1987; Kunhardt and Tzeng, 1988; Wang and Kunhardt, 1990; Eliasson and Kogelschatz, 1991a). These studies promoted the industrial use of pulsed plasma. However, further study on the pulsed plasma is still required since the discharge feature of a plasma depends on the kind of plasma, the background gas, electrode arrangement, and some unknown factors.

Direct methane conversion to more valuable chemicals and liquid fuels has attracted much more attention from the beginning of 1980s (Edwards and Foster, 1986; Spencer and Pereira, 1987; Renesme et al., 1992; Fierro, 1993; Fox, 1993; Krylov, 1993; Parkyns et al., 1993; Arutyunov et al., 1996). Catalytic selective oxidation of methane to methanol was expected to be able to obviously save investment and operation cost if methane conversion and methanol selectivity can reach high levels. Since methanol can be oxidized over a catalyst (Taylor et al., 1995), some improvements were made, such as using a catalytic reactor operated with a very short contact time to prevent methanol from deep oxidation (Deutschmann and Schmidt, 1998). However, we found that even SiO_2 that is usually used as an inert support of a catalyst can oxidize the product methanol to formaldehyde, CO, and CO_2 at a reaction temperature higher than 500°C (Yao et al., 2000c). This suggested that the catalytic selective oxidation of

Correspondence concerning this article should be addressed to E. Suzuki.

methane to methanol is confronted with a contradiction of keeping high methanol selectivity at a high methane conversion for its industrial application.

Methane conversion using a plasma has been studied for many years. AC and DC corona discharges, dielectric-barrier discharge, arc plasma, and the combination of microwave plasma and catalysts have been reported to produce acetylene, ethylene, hydrogen, methanol, and other liquid products (Wan, 1986; Mallinson et al., 1987; Bhatnagar and Mallinson, 1995; Liu et al., 1996; Thanyachotpaiboon et al., 1998; Onoe et al., 1997; Okumoto et al., 1998; Suib and Zerger, 1993; Marun et al., 1999; Eliasson et al., 2000; Yao et al., 2000d). Recently, methane reforming with CO_2 using plasmas, which may contribute to effective utilization of methane and reduction of greenhouse gas CO_2 emission, has been reported (Gesser et al., 1997; Bromberg et al., 1998; Larkin et al., 1998; Zhou et al., 1998; Huang et al., 2000; Yao et al., 2000b).

Methane conversion using an arc plasma was reported with a high electric efficiency (Gladisch, 1962; Fey, 1979). The arc plasma process has some shortcomings such as the extremely high temperature (several thousand degrees centigrade) and carbon deposition in the plasma zone. A DC pulse discharge was used to reduce carbon deposition with Ar dilution and oxidation, but its energy efficiency is less than 5% of that of DC arc plasma, and this DC pulse discharge is, therefore, not feasible for methane conversion (Kado et al., 1999). Other kinds of plasma, such as AC and DC corona discharges, microwave plasma, and low-frequency pulsed plasma, have a low energy efficiency and still should be further studied.

We have found that a nonthermal pulsed plasma with a high pulse frequency can be used to convert methane to acetylene, which will be described in detail in a future publication (Yao et al., 2000a). Methane can be converted to acetylene at a high acetylene selectivity and high methane conversion at room temperature and atmospheric pressure by the high-frequency pulsed plasma, indicating that the high-frequency pulsed plasma is competitive with the commercial acetylene production processes. Therefore, fundamentals of such a high-frequency pulsed plasma is required to be investigated for its industrialization. However, the pulsed plasma has been carried out conventionally at a frequency of less than 1 kPPS (Gallimberti, 1988; Hall, 1990; Rea and Yan, 1993; Creyghton et al., 1993; Smulders et al., 1998), and that at a frequency higher than 1 kPPS has not been explored. In this study, we investigated the pulsed plasma of methane at single and sequential high-frequency pulse modes.

Experimental Setup

Figure 1 shows the apparatus with a pulse power supply and reactor. The pulse power was generated with a pulse power supply DP-15K35, which Pulse Electronic Engineering constructed according to our specifications. A hydrogen thyratron (CX1535S, EEV) was used as a switch, and its modulation by a driver was applied to control the pulse frequency. The pulse voltage was adjusted via the input voltage of the charging system (CS) for plasma forming capacitors. This input voltage was named as CS input voltage in this study. The rise rate of voltage and duration time were 0.5–0.6 $kV \cdot ns^{-1}$ and 700 ns under the condition without loads, respectively. Discharge currents through anode and cathode

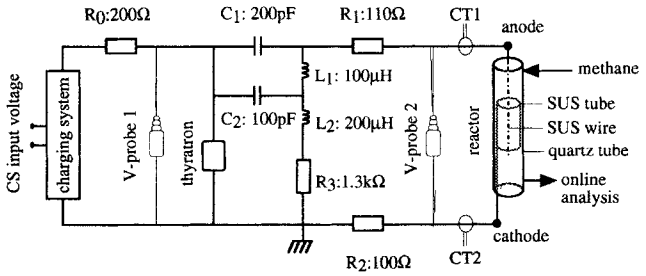

Figure 1. Pulse power supply and reactor.

were measured with two current transformers (CT1, mode 2–1.0, 35 MHz; CT2, Mode 0.5–1.0, 20 MHz, Strangenes Industries) and the discharge voltage was measured with a voltage probe (V-probe 2, EP-50K, 50 MHz, Pulse Electronic Engineering). The signals from the voltage probe and current transformers were recorded with a digital oscilloscope (TDS754D, Tektronix) having an analog bandwidth of 500 MHz and a maximum sampling rate of 2×10^9 samples per second. The reactor consisted mainly of a quartz tube (12 mm i.d., 150 mm o.d., and 500 mm length), a stainless steel tube (SUS 316, cathode, 10 mm i.d., 12 mm o.d., and 150 mm length), and a stainless steel wire (SUS 316, anode, Φ 0.5 mm). The stainless steel tube and wire were set in the central part of the quartz tube.

Methane was introduced into the upper part of the vertically placed reactor. Hydrocarbons from the lower part of the reactor were analyzed with an online chromatograph (GC 103, Okura Riken, FID) equipped with a 2 m Porapak N column. All experiments were carried out at room temperature and atmospheric pressure.

A point-plate reactor and ultra high-speed digital imaging system (IMACON 468, Hadland) were used for imaging analysis (Figure 2). Six images were sequentially taken without intervals with an exposure time of 10 ns for each image. The exposure timing of the first image was controlled by a pretrigger signal from the pulse power supply. The influence of each signal cable (V-probe, CT1, CT2, and TTL from IMACON 468) on signal delay recorded with the digital oscilloscope was corrected so that the position of each image could be exactly decided.

The energy injection rates in J/PPS (pulse per second) into the background methane gas were designated as P_a and P_c for anode and cathode, respectively. P_a and P_c were calculated by Eqs. 1 and 2, respectively, from pulse voltage V_i in volts and anode current I_{ai} and cathode current I_{ci} in am-

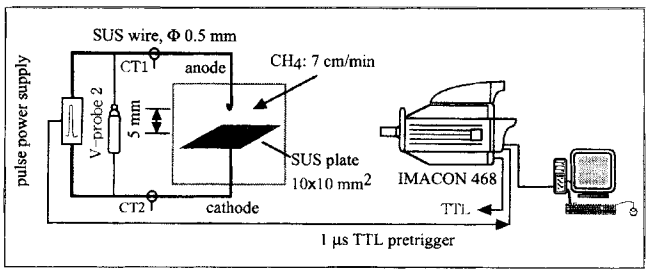

Figure 2. Imaging system.

peres at discharge time t_i in seconds

$$P_a = \Sigma((V_i + V_{i+1})/2)((I_{ai} + I_{ai+1})/2)(t_{i+1} - t_i) \quad (1)$$

$$P_c = \Sigma((V_i + V_{i+1})/2)((I_{ci} + I_{ci+1})/2)(t_{i+1} - t_i) \quad (2)$$

The energy W charged into the capacitors was given by $W = 0.5C_tV_p^2$ in J/PPS. Here, C_t is total capacitance of plasma forming capacitors C1 and C2 in Farads. V_p is 68.8 times as much as CS input voltage. The energy efficiencies of the capacitors for discharge, η_a and η_c, were calculated from anode and cathode currents by Eqs. 3 and 4, respectively.

$$\eta_a = P_a/W \quad (3)$$

$$\eta_c = P_c/W \quad (4)$$

The electric charges that flowed through the discharge gap were calculated from anode and cathode currents as follows

$$Q_a = \Sigma((I_{ai} + I_{ai+1})/2)(t_{i+1} - t_i) \quad (5)$$

$$Q_c = \Sigma((I_{ci} + I_{ci+1})/2)(t_{i+1} - t_i) \quad (6)$$

Using the total electric charges into the capacitors, $Q = C_tV_p$, the charge balance ζ_a and ζ_c based on anode and cathode currents, respectively, were calculated as follows

$$\zeta_a = Q_a/Q \quad (7)$$

$$\zeta_c = Q_c/Q \quad (8)$$

The conversion rate of methane R in mol/J was defined as: moles of methane converted in a minute /(60 F P_a). Here, F is the pulse frequency in PPS.

Results and Discussion

Pulsed plasma of methane with a single pulse mode

We first measured the waveforms of discharge voltage and currents with the single pulse mode. At a CS input voltage of 130 V, the discharge voltage increased to a peak value and then decreased gradually (Figure 3). A sharp peak occurred simultaneously with the rise of the discharge voltage in the waveforms and anode and cathode currents. This sharp peak was partially due to the stray capacitors (about 10 to 15 pF, resulting in 6–9 A current at maximum) of the reactor side circuit between two current transformers, and mainly due to the discharge defined as a pulsed corona discharge (about 10 A) in this study. It is also called streamer corona discharge (Sigmond, 1984), or primary streamer discharge (Marode, 1975). The anode current was higher than the cathode current (less than 6 A). This implied that ions were formed in the pulsed corona discharge that might obey the Townsend criterion. Relatively flat and similar peaks were found following the pulsed corona discharge in both anode and cathode current waveforms. These correspond to a pulsed streamer

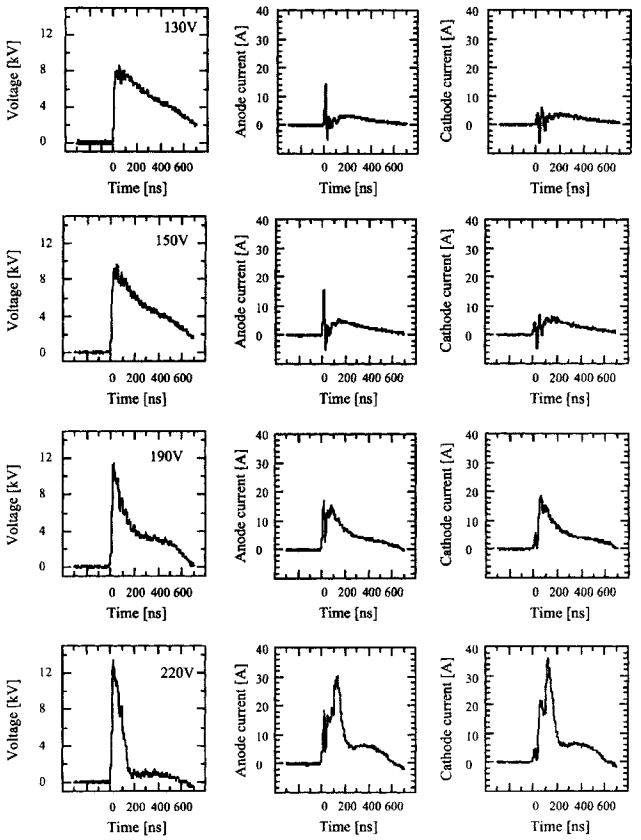

Figure 3. Waveforms of discharge voltage and currents at various CS input voltages.

Methane was supplied at a flow rate of 150 mL/min at room temperature and atmospheric pressure.

discharge. The pulsed streamer discharge became stronger as the CS input voltage increased (Figure 3, 150 V and 190 V). Finally, a pulsed spark discharge developed at a CS input voltage of 220 V (Figure 3, 220 V). The current waveform of anode was also the same as that of cathode in the pulsed spark discharge period. These findings suggested that the pulsed streamer and spark discharges are largely resistive as suggested by Spitzer (1962) and Marode (1975). The resistance in the pulsed streamer discharge, which was calculated as the ratio of discharge voltage to anode current, was at a level of 2,000 Ω at a CS input voltage of 130 V.

The streak image of methane pulsed plasma at atmospheric pressure is shown in Figure 4 together with the waveforms of discharge voltage and currents (Figure 5) using the experimental setup in Figure 2. Images in Figures 4a and 4b represent the pulsed corona discharge. In the first half period of the pulsed corona discharge, no detectable luminescence emission was found, but in the latter, a brush pulsed corona discharge with relatively weak emission of light was observed. The strength of the brush branch increased in the pulsed streamer (Image c) and resulted in a completely bridged streamer (Image d). Images e and f show the pulsed spark discharge emitting extremely strong light. In this study the discharge between a short gap is bridged. This is due to the characteristics of methane and electrode arrangement

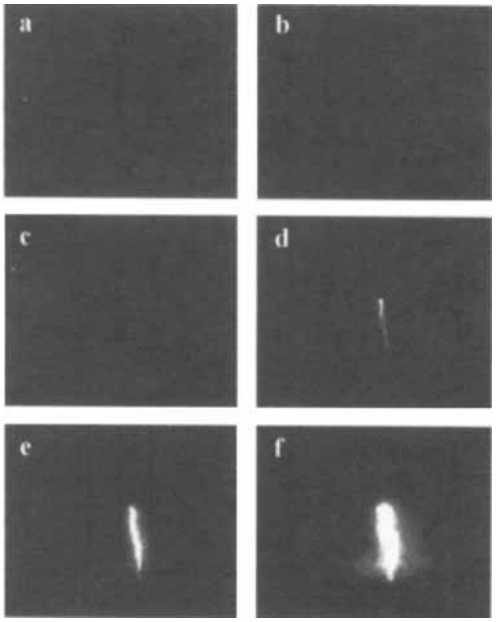

Figure 4. Pulsed plasma at different imaging periods (Figure 6) between a point-plate gap.

Methane was supplied at a velocity of 7 cm/min at room temperature and atmospheric pressure.

since the pulsed streamer discharges of air between a long gap of 140–150 mm (Smulders et al., 1998) and 15 mm (Marode, 1975) were not completely bridged.

The energy injection rate into methane was then calculated by equations 1 and 2. The energy injection rate in a pulsed corona discharge period was less than 3 mJ/PPS, which was 1/6–1/8 of the total injection rate (Figure 6). The injection rate lasted for 600 ns due to the pulsed streamer discharge. The injection rate increased with the increase in CS input voltage with a small downturn between 200 V and 210 V

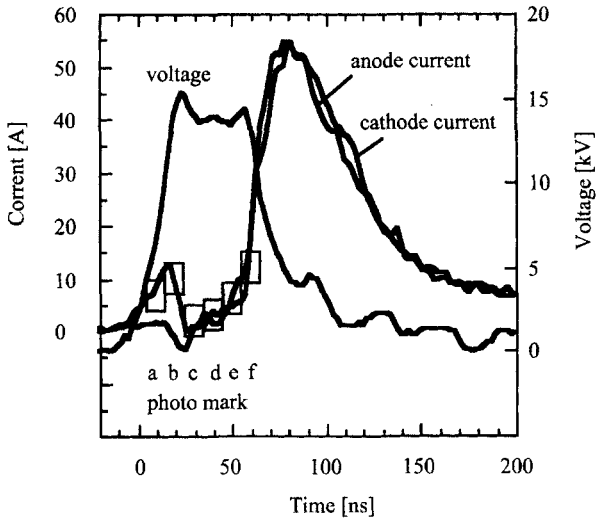

Figure 5. Imaging period for each image.

Exposure time of each rectangle was 10 ns.

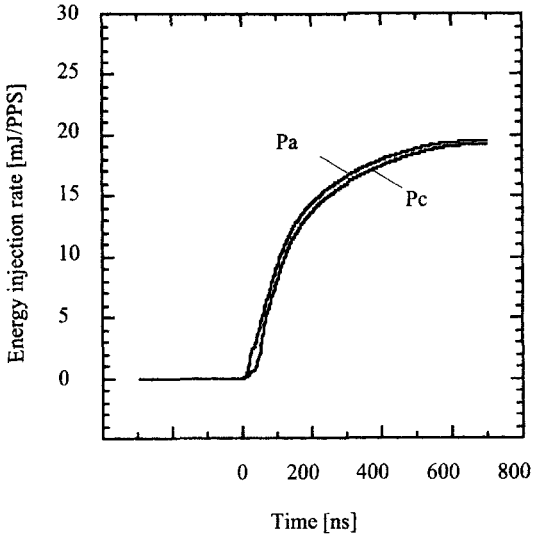

Figure 6. Energy injection rate according to discharge time at 190 V CS input with the single pulse mode.

Conditions are the same as those in Figure 3.

(Figure 7). This downturn is due to the decrease in resistance of background gas of methane. The energy efficiency of the capacitors for discharge peaked at a CS input voltage of 180 V (Figure 8). The low efficiency at a CS input voltage lower than 180 V is due to the side path current through the resistor R3 and inductors L1 and L2. The decrease in energy efficiency at a CS input voltage higher than 180 V is due to the decrease in resistance of the discharge gap. The electric charge balance calculated with Eqs. 5 and 6 is shown in Figure 9. The electric charge balance was less than 100% at a CS input voltage less than 190 V also due to the side path of

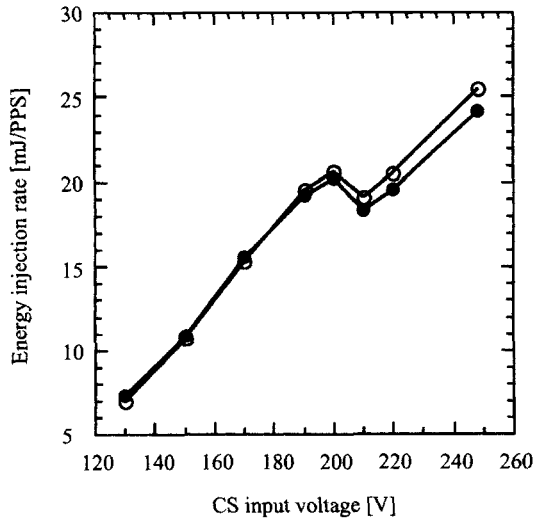

Figure 7. Energy injection rate at various CS input voltages with the single pulse mode.

Conditions are the same as those in Figure 3. ○— P_a; ●— P_c.

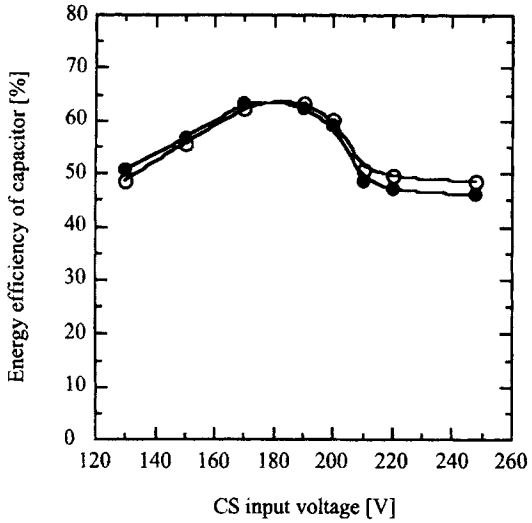

Figure 8. Energy efficiency of the capacitor at various CS input voltages.

Conditions are the same as those in Figure 3. ○— η_a; ●— η_c.

R3, L1, and L2. The electric charge balance was higher than 100% if the stray capacitance was not considered. This indicated that the total stray capacitance was about 60 pF, including 10 pF from V-probe 1 and 10 to 15 pF from the reactor side stray capacitors.

High frequency pulsed plasma of methane

We then measured the waveforms of discharge voltage and currents at a CS input voltage of 130 V and pulse frequency of 1, 4, 6, or 8 kpps (Figure 10). At 1 kPPS, the discharge

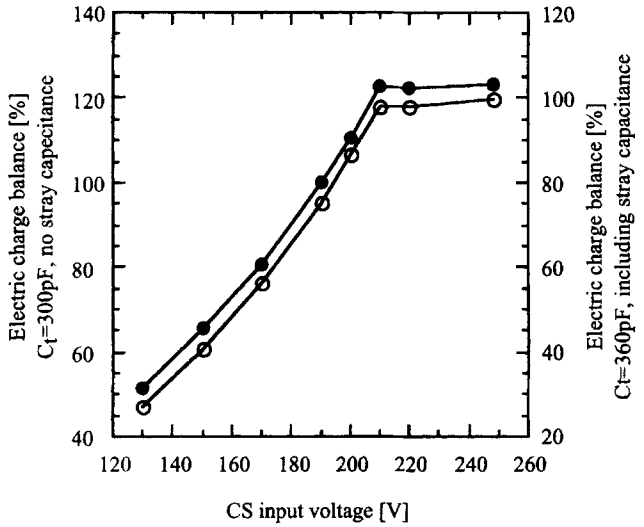

Figure 9. Electric charge balance at various CS input voltages.

Left vertical axis: calculated without consideration of the existence of stray capacitors; right vertical axis: calculated with consideration of the existence of stray capacitors. Conditions are the same as those in Figure 3. ○— ζ_a; ●— ζ_c.

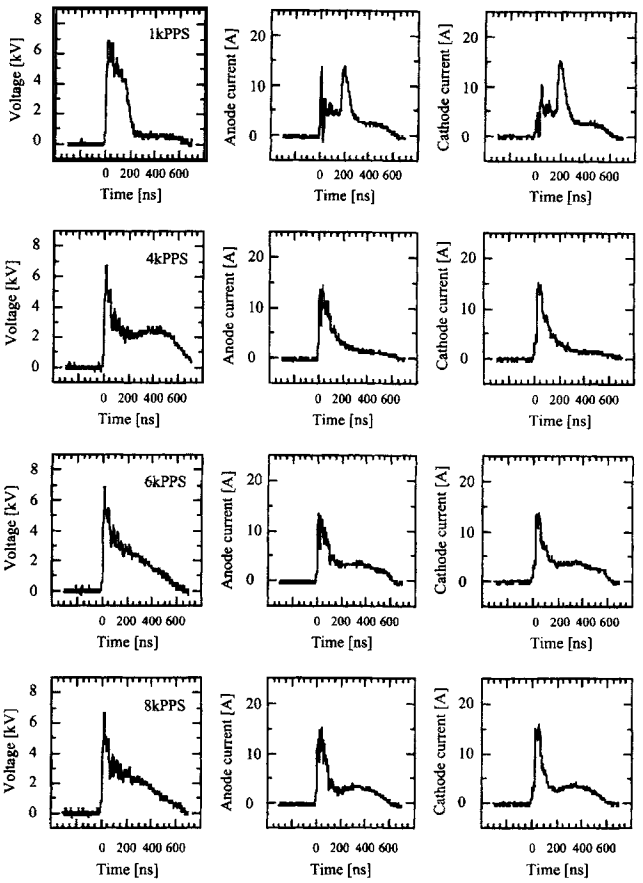

Figure 10. Waveforms of discharge voltage and currents at various pulse frequencies with the sequential pulse mode at 130 V CS input.

Methane was supplied at a flow rate of 150 mL/min at room temperature and atmospheric pressure.

voltage rose to a peak value, then decreased gradually before 190 ns but rapidly dropped to 500 V in the discharge time of 190–210 ns. This rapid voltage drop was due to the pulsed streamer or spark discharge which could be found in the waveforms of anode and cathode currents. This pulsed streamer or spark discharge was obviously ascribed to the repetition of pulsed corona and streamer discharges since only pulsed corona and streamer discharges could be found from the waveforms at a single pulse mode (Figure 3, 130 V). The pulsed corona, streamer, and spark discharges occurred sequentially and finally trended to assimilate each other when the pulse frequency increased. These findings implied that ions in the plasma zone could contribute to the formation of next pulsed streamer or spark discharge.

The electric charge balance shown in Figure 11 was markedly higher than at at a single pulse mode (Figure 9). This indicated that most electric charges flowed through the discharge gap due to the decrease in resistance of background methane gas to a level of 500–1,000 Ω at a CS input voltage of 130 V and 8 kpps. Although the energy efficiency of the capacitors for the discharge (Figure 12) was at the same level as that at a single pulse mode (Figure 8), the mechanism is different. At a single pulse mode, the low electric

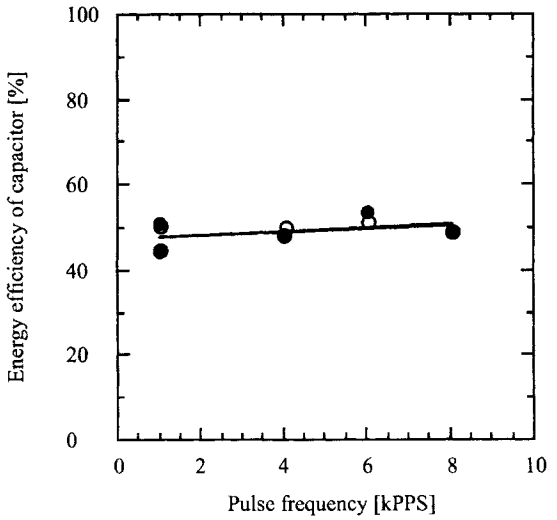

Figure 11. Electric charge balance at various pulse frequencies with the sequential pulse mode at 130 V CS input.

Conditions are the same as those in Figure 10. ○—ζ_a; ●—ζ_c.

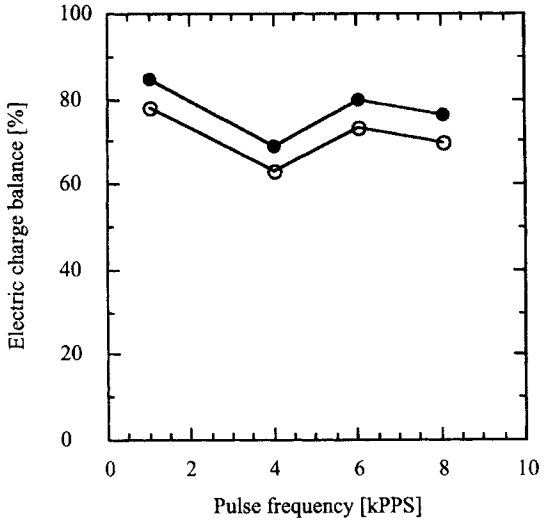

Figure 12. Energy efficiency at various pulse frequencies with the sequential pulse mode at 130 V CS input.

Conditions are the same as those in Figure 10. ○—η_a; ●—η_c.

charge balance (Figure 9) explained that energy loss is due to the side path of R3, L1, and L2. At a sequential pulse mode, the energy loss is due to the above side path and resistors of R1 and R2 in the main discharge circuit. Therefore, on the principle of electronics, the energy efficiency of the capacitor could be further improved by increasing the resistance of the background gas and R3 or decreasing the resistance of R1 and R2.

Reactivity of the high frequency pulsed plasma

Methane activation in the pulsed plasma using a gradual dehydrogenation mode can be written as follows

$$CH_4 + e \rightarrow CH_x + (4-x)H + e \quad (x = 0\text{–}3) \qquad (9)$$

The main products are acetylene, ethylene, ethane, and hydrogen. The selectivity of hydrogen was 100% in all experiments. These products are produced directly from a combination of CH_3, CH_2, and CH radicals. Acetylene and ethylene can be also from the dehydrogenation of ethylene and ethane, respectively. In order to evaluate the reactivity of such a pulsed plasma, we calculated the methane conversion rate at 1 and 8 kpps. The results are shown in Figure 13 together with the methane conversion rates with other kinds of plasmas. The methane conversion rate at 8 kPPS is lower than that using arc plasma, but higher than those of microwave (Suib and Zerger, 1993), silent plasmas, (Shepelev et al., 1993; Larkin et al., 2000), and even the high frequency pulsed plasma of a mixture of methane and carbon dioxide (Yao et al., 2000b).

Conclusions

We have experimentally characterized pulsed plasma of methane using single and sequential pulse modes.

At a single pulse mode, only pulsed corona and streamer discharges were found at a low CS input voltage. A pulsed spark discharge was observed following the pulsed streamer discharge at a high CS input voltage. In the latter period of pulsed corona discharge, a weak emission of light was found using image analysis. The pulsed streamer and spark discharges then developed after the pulsed corona discharge. The pulsed streamer and spark discharges were resistive. Most of the energy was injected within these two discharges.

At a sequential pulse mode, the discharge became easier as the pulse frequency increased even at a low CS input voltage. This implied that the pulsed plasma could be realized at a relative low pulse voltage and high pulse frequency. The energy efficiency was about 50% at a CS input voltage of 130

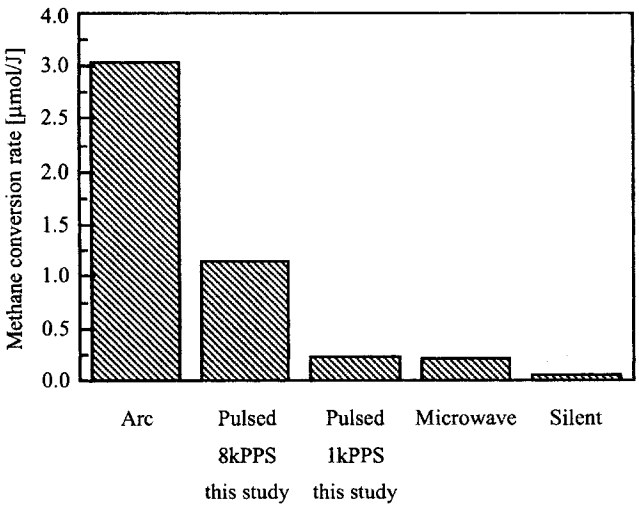

Figure 13. Comparison of methane conversion rate with some other kinds of plasmas.

V. The energy efficiency could be further improved by increasing resistance of R3 and decreasing resistance of R1 and R2. The methane conversion rate at a high frequency, which indicates the energy efficiency of the pulsed plasma, was dramatically increased by three-fold compared to that at a low pulse frequency. This methane conversion rate is higher than those of microwave and silent plasmas. The high-frequency pulsed plasma is more practical than the arc plasma since the pulsed plasma can be carried out at room temperature, but the arc plasma usually can be carried out only at an extremely high temperature.

Our results showed that the pulsed plasma at a high frequency easily occurred possibly due to the existence of ions in the plasma zone. These ions formed in the former pulse period could contribute to the formation of the next pulsed plasma. Thus, there is a close relation between single and sequential pulsed plasmas. This relation will be further studied.

Since the high-frequency pulsed plasma has a high energy efficiency, we suggest that such a novel pulsed plasma is also useful for other applications such as decomposition of environmental pollutants.

Acknowledgments

This study was supported by the New Energy and Industrial Technology Development Organization (NEDO) and Nara Institute of Science and Technology.

Literature Cited

Arutyunov, V. S., V. Ya. Basevich, and V. I. Vedeneev, "Direct High-Pressure Gas-Phase Oxidation of Natural Gas to Methanol and Other Oxygenates," *Russian Chem. Rev.*, **65**, 197 (1996).

Bhatnagar, R., and R. G. Mallinson, *Methane and Alkane Conversion Chemistry*, Plenum Press, New York (1995).

Bromberg, L., D. R. Cohn, A. Rabinovich, C. O'Brien, and S. Hochgreb, "Plasma Reforming of Methane," *Energy Fuels*, **12**, 11 (1998).

Chang, J. S., "Energetic Electron Induced Plasma Processes for Reduction of Acid and Greenhouse Gases in Combustion Flue Gas," *NATO ASI Series G*, **34**, 1 (1993).

Creyghton, Y. L. M., E. M. van Velghuizen, and W. R. Rutgers, "Electrical and Optical Study of Pulsed Positive Corona," *NATO Series G*, **34**, 205 (1993).

Dawson, G. A., and W. P. Winn, "A Model for Streamer Propagation," *Zeitschrift für Physik*, **183**, 159 (1965).

Deutschmann, O., and L. D. Schmidt, "Modeling the Partial Oxidation of Methane in a Short Contact Time Reactor," *AIChE J.*, **44**, 2465 (1998).

Dhali, S. K., and P. F. Williams, "Numerical Simulation of Streamer Propagation in Nitrogen at Atmospheric Pressure," *Phys. Rev. A*, **2**, 1219 (1985).

Dhali, S. K., and P. F. Williams, "Two-Dimensional Studies of Streamers in Gases," *J. Appl. Phys.*, **62**, 4696 (1987).

Edwards, J. H., and N. R. Foster, "The Potential for Methanol Production from Natural Gas by Direct Catalytic Partial Oxidation," *Fuel Sci. Technol. INT'L.*, **4**, 365 (1986).

Eliasson, B., C.-L. Liu, and U. Kogelschatz, "Direct Conversion of Methane and Carbon Dioxide to Higher Hydrocarbons Using Catalytic Dielectric-Barrier Dischargers with Zeolites," *Ind. Eng. Chem. Res.*, **39**, 1221 (2000).

Eliasson, B., and U. Kogelschatz, "Modeling and Applications of Silent Discharge Plasmas," *IEEE Trans. Plasma Sci.*, **19**, 309 (1991a).

Eliasson, B., and U. Kogelschatz, "Nonequilibrium Volume Plasma Chemical Processing," *IEEE Trans. Plasma Sci.*, **19**, 1063 (1991b).

Fey, M. G., "Arc Heater Pyrolysis of Hydrocarbons," AIChE Meeting, Paper 35C, Philadelphia, PA (1979).

Fierro, J. L. G., "Catalysis in C1 Chemistry: Future and Prospect," *Catal. Lett.*, **22**, 67 (1993).

Fox, J. M., "The Different Catalytic Routes for Methane Valorization: An Assessment of Processes for Liquid Fuels," *Catal. Rev. Sci. Eng.*, **35**, 169 (1993).

Gallimberti, I., "Impulse Corona Simulation for Flue Gas Treatment," *Pure Appl. Chem.*, **60**, 663 (1988).

Geary, J. M., and G. W. Penney, "Charged-Sheath Model of Cathode-Directed Streamer Propagation," *Phys. Rev. A*, **17**, 1483 (1978).

Gesser, H. D., N. R. Hunter, and D. Probawono, "The CO_2 Reforming of Natural Gas in a Silent Discharge Reactor," *Plasma Chem. Plasma Process.*, **18**, 241 (1997).

Gladisch, H., "How Hüels Makes Acetylene by DC Arc," *Hydrocarbon Process. Petrol. Refiner*, **41**, 159 (1962).

Hall, H. J., "History of Pulse Energization in Electrostatic Precipitation," *J. Electrostatics*, **25**, 1 (1990).

Horvath, M., L. Bilitzky, and J. Huttner, *Ozone*, Elsevier, New York (1985).

Huang, A., G. Xia, J. Wang, S. L. Suib, Y. Hayashi, and H. Matsumoto, "CO_2 Reforming of CH_4 by Atmospheric Pressure AC Discharge Plasmas," *J. Catal.*, **189**, 349 (2000).

Kado, S., Y. Sekine, and K. Fujimoto, "Direct Synthesis of Acetylene from Methane by Direct Current Pulse Discharge," *Chem. Comm.*, **24**, 2485 (1999).

Krylov, O. V., "Catalytic Reaction of Partial Methane Oxidation," *Catal. Today*, **18**, 209 (1993).

Kunhardt, E. E., and Y. Tzeng, "Development of an Electron Avalanche and Its Transition into Streamer," *Phys. Rev. A*, **38**, 1410 (1988).

Larkin, D. W., T. A. Caldwell, L. L. Lobban, and R. G. Mallinson, "Oxygen Pathways and Carbon Dioxide Utilization in Methane Partial Oxidation in Ambient Temperature Electric Discharges," *Energy Fuels*, **12(4)**, 740 (1998).

Larkin, D. W., L. L. Lobban, and R. G. Mallinson, "Production of Organic Oxygenates in the Partial Oxidation of Methane in a Silent Electric Discharge Reactor," First International Conference on Gas Processing, AIChE Meeting, 10 (2000).

Liu, C. G., A. Marafee, B. J. Hill, G. H. Xu, R. Mallinson, and L. Lobban, "Oxidative Coupling of Methane with AC and DC Corona Discharges," *Ind. Eng. Chem. Res.*, **35**(10), 3295 (1996).

Mallinson, R. G., C. M. Sliepcevich, and S. Rusek, "Methane Partial Oxidation in Alternating Electric Fields," *Am. Chem. Soc., Div. Fuel Chem.*, **32**, 266 (1987).

Marode, E., "The Mechanism of Spark Breakdown in Air at Atmospheric Pressure between a Positive Point and a Plane, I. Experimental," *J. Appl. Phys.*, **46**, 2005 (1975).

Marun, C., L. D. Conde, and S. L. Suib, "Catalytic Oligomerization of Methane via Microwave Heating," *J. Phys. Chem. A*, **103**, 4332 (1999).

Mutaf-Yardimchi, O., L. A. Kennedy, S. A. Nester, A. V. Saveliev, and A. A. Fridman, "Plasma-Catalytic Treatment of Organic Compounds in Atmospheric Pressure Non-Equilibrium Discharges," SAE 982427 (1998).

Oda, T., T. Kato, T. Takahashi, and K. Shimizu, "Nitric Oxide Decomposition in Air Using Nonthermal Plasma Processing with Additives and Catalyst," *IEEE Trans. Ind. Appl.*, **34(2)**, 268 (1998).

Okumoto, M., B. S. Rajanikanth, S. Katsura, and A. Mizuno, "Nonthermal Plasma Approach in Direct Methanol Synthesis from CH_4," *IEEE Trans. Ind. Appl.*, **34**, 940 (1998).

Onoe, K., A. Fujie, T. Yamaguchi, and Y. Hatano, "Selective Synthesis of Acetylene from Methane by Microwave Plasma Reactions," *Fuel*, **76**, 281 (1997).

Parkyns, N. D., C. I. Warburton, and J. D. Wilson, "Natural Gas Conversion to Liquid Fuels and Chemicals: Where Does It Stand?," *Catal. Today*, **18**, 385 (1993).

Penetrante, B. M., M. C. Hsiao, J. N. Bardsley, B. T. Merritt, G. E. Vogtlin, A. Kuthi, C. P. Burkhart, and J. R. Bayless, "Identification of Mechanisms for Decomposition of Air Pollutants by Non-Thermal Plasma Processing," *Plasma Sources Sci. Technol.*, **6**, 251 (1997).

Potakin, B. V., M. A. Deminsky, A. A. Fridman, and V. D. Rusanov, "The Effect of Clusters and Heterogeneous Reactions on Non-Equilibrium Plasma Flue Gas Cleaning," *NATO ASI Series G*, **34**, 91 (1993).

Puchkarev, V., G. Roth, and M. Gundersen, "Plasma Processing of Diesel Exhaust by Pulsed Corona Discharge," SAE 982516 (1988).
Rea, M., and K. Yan, "Energization of Pulse Corona Induced Chemical Processes," *NATO Series G*, **34**, 191 (1993).
Renesme, G., J. Saint-Just, and Y. Muller, "Transportation Fuels and Chemicals Directly from Natural Gas: How Expensive?," *Catal. Today*, **13**, 371 (1992).
Shepelev, S. S., H. D. Gesser, and N. R. Hunter, "Light Paraffin Oxidative Conversion in a Silent Electric Discharge," *Plasma Chem. Plasma Process.*, **13**, 479 (1993).
Sigmond, R. S., "The Residual Streamer Channel: Return Strokes and Secondary Streamers," *J. Appl. Phys.*, **56**, 1355 (1984).
Smulders, E. H. W. M., B. E. J. M. van Heesch, and S. S. V. B. van Paasen, "Pulsed Power Corona Discharges for Air Pollution Control," *IEEE Trans. Plasma Sci.*, **26**, 1476 (1998).
Spencer, N. D., and C. J. Pereira, "Partial Oxidation of CH_4 to HCHO over a MoO_3-SiO_2 Catalyst: A Kinetic Study," *AIChE J.*, **33**, 1808 (1987).
Spitzer, L., *Physics of Fully Ionized Gases*, Interscience Publishers, New York (1962).
Suib, S. L., and R. P. Zerger, "A Direct, Sequential, Low-Power Catalytic Conversion of Methane to Higher Hydrocarbons via Microwave Plasmas," *J. Catal.* **139**, 383 (1993).
Sun, B., M. Sato, and J. S. Clements, "Use of a Pulsed High-Voltage Discharge for Removal of Organic Compounds in Aqueous Solution," *J. Phys. D: Appl. Phys.*, **32**, 1908 (1999).
Taylor, S. H., J. S. J. Hargreaves, G. J. Hutchings, and R. W. Joyner, *Methane and Alkane Conversion Chemistry*, Plenum Press, New York (1995).
Thanyachotpaiboon, K., S. Chavadej, T. A. Caldwell, L. L. Lobban, and R. G. Mallinson, "Conversion of Methane to Higher Hydrocarbons in AC Nonequilibrium Plasmas," *AIChE J.*, **44**, 2252 (1998).
Urashima, K., X. Tong, J. S. Chang, A. Miziolek, and L. A. Rosocha, "Acid Gas Removal Characteristics of Corona Discharge Methane Radical Shower-Catalyst Hybrid System for Treatment of Jet Engine Test Cell Flue Gas," SAE 99-01-3634 (1999).
Wan, J. K. S., "Microwave Induced Catalytic Conversion of Methane to Ethylene and Hydrogen," U.S. Patent No. 4574038 (1986).
Wang, M. C., and E. E. Kunhardt, "Streamer Dynamics," *Phys. Rev. A*, **42**, 2366 (1990).
Yao, S. L., A. Nakayama, and E. Suzuki, "Methane Conversion Using a High-Frequency Pulsed Plasma: Important Factors," *AIChE J.*, in press (2000a).
Yao, S. L., F. Ouyang, A. Nakayama, E. Suzuki, M. Okumoto, and A. Mizuno, "Oxidative Coupling and Reforming of Methane with Carbon Dioxide Using a High-Frequency Pulsed Plasma," *Energy Fuels*, **14**, 910 (2000b).
Yao, S. L., F. Ouyang, S. Shimumora, H. Sakurai, K. Tabata, and E. Suzuki, "A Kinetic Study of Methanol Oxidation over SiO_2," *Appl. Catal. A: General*, **198**, 43 (2000).
Yao, S. L., T. Takemoto, F. Ouyang, A. Nakayama, E. Suzuki, A. Mizuno, and M. Okumoto, "Selective Oxidation of Methane Using a Non-Thermal Pulsed Plasma," *Energy Fuels*, **14**, 459 (2000).
Zhou, L. M., B. Xue, U. Kogelshatz, and B. Eliasson, "Nonequilibrium Plasma Reforming of Greenhouse Gases to Synthesis Gas," *Energy Fuels*, **12**, 1191 (1998).

Manuscript received Mar. 6, 2000, and revision received July 3, 2000.